ARMY RESEARCH LABORATORY

A Molecular Dynamics Study of Detonation: I. A Comparison With Hydrodynamic Predictions

Betsy M. Rice
William Mattson
John Grosh
U.S. ARMY RESEARCH LABORATORY

S. F. Trevino
U.S. ARMY ARMAMENT RESEARCH, DEVELOPMENT, & ENGINEERING CENTER
AND NATIONAL INSTITUTE OF STANDARDS AND TECHNOLOGY

19960318 051

NOTICES

REPORT DOCUMENTATION PAGE

Form Approved
OMB No. 0704-0188

Public reporting burden for this collection of information is estimated to average 1 hour per response, including the time for reviewing instructions, searching existing data sources, gathering and maintaining the data needed, and completing and reviewing the collection of information. Send comments regarding this burden estimate or any other aspect of this collection of information, including suggestions for reducing this burden, to Washington Headquarters Services, Directorate for Information Operations and Reports, 1215 Jefferson Davis Highway, Suite 1204, Arlington, VA 22202-4302, and to the Office of Management and Budget, Paperwork Reduction Project(0704-0188), Washington, DC 20503.

1. AGENCY USE ONLY *(Leave blank)*	2. REPORT DATE March 1996	3. REPORT TYPE AND DATES COVERED Final, Jan 94 - Aug 95

4. TITLE AND SUBTITLE
A Molecular Dynamics Study of Detonation: I. A Comparison With Hydrodynamic Predictions

5. FUNDING NUMBERS
PR: 1L161102AH43

6. AUTHOR(S)
Betsy M. Rice, William Mattson, John Grosh, and S. F. Trevino*

7. PERFORMING ORGANIZATION NAME(S) AND ADDRESS(ES)
U.S. Army Research Laboratory
ATTN: AMSRL-WT-PC
Aberdeen Proving Ground, MD 21005-5066

8. PERFORMING ORGANIZATION REPORT NUMBER
ARL-TR-981

9. SPONSORING/MONITORING AGENCY NAMES(S) AND ADDRESS(ES)

10. SPONSORING/MONITORING AGENCY REPORT NUMBER

11. SUPPLEMENTARY NOTES
*U.S. Army Armament Research, Development, and Engineering Center, Picatinny Arsenal, NJ 07806, and National Institute of Standards and Technology, Gaithersburg, MD 20899.

12a. DISTRIBUTION/AVAILABILITY STATEMENT

Approved for public release; distribution is unlimited.

12b. DISTRIBUTION CODE

13. ABSTRACT *(Maximum 200 words)*

We have compared the predictions of hydrodynamic theory for the properties of an unsupported detonation with the results of a molecular dynamics simulation of such a phenomenon. The model of an energetic crystal consists of heteronuclear diatomic molecules which require energy to break the molecular bonds (at ambient pressure) and release substantial energy upon association of the products to form homonuclear diatomic molecules. The equation of state used in the hydrodynamic theory is determined from two-dimensional molecular dynamics simulations of this model at various equilibrium conditions corresponding to volumes and temperatures appropriate to the detonation. The Chapman-Jouguet conditions of detonation were thus determined. The properties of the detonation were subsequently measured directly from two-dimensional molecular dynamics simulations of the crystal model subjected to shock initiation. The agreement between the hydrodynamic predictions and the measured properties is good. Deviations from exact agreement are attributed to slight differences in material composition in the detonation simulation compared to that of the equation-of-state calculations. The critical property for sustained detonation using this model appears to be the attainment of the Chapman-Jouguet density.

14. SUBJECT TERMS
molecular dynamics, hydrodynamic theory, detonation, Monte Carlo

15. NUMBER OF PAGES
39

16. PRICE CODE

17. SECURITY CLASSIFICATION OF REPORT	18. SECURITY CLASSIFICATION OF THIS PAGE	19. SECURITY CLASSIFICATION OF ABSTRACT	20. LIMITATION OF ABSTRACT
UNCLASSIFIED	UNCLASSIFIED	UNCLASSIFIED	UL

NSN 7540-01-280-5500

Standard Form 298 (Rev. 2-89)
Prescribed by ANSI Std. 239-18   298-102

INTENTIONALLY LEFT BLANK.

ACKNOWLEDGMENTS

INTENTIONALLY LEFT BLANK.

TABLE OF CONTENTS

INTENTIONALLY LEFT BLANK.

LIST OF FIGURES

INTENTIONALLY LEFT BLANK.

LIST OF TABLES

INTENTIONALLY LEFT BLANK.

1. INTRODUCTION

The field of detonation physics has enjoyed considerable attention since the phenomenon was recognized over a century ago (Berthelot and Vielle 1881, 1882a, 1882b; Mallard and LeChatelier 1881). Benefits that would result from the ability to exploit and control such energetic events have led to numerous explorations designed to determine the character of a system and conditions that will result in a detonation. The extreme pressures and high energies released in a detonation have posed considerable experimental challenges toward these characterizations. Even greater obstacles in monitoring detailed microscopic chemical and physical changes in the detonation are the time and length scales over which the event occurs. These experimental challenges have necessitated development of theories that attempt to describe the phenomenon and complement the experimental analyses. The majority of theoretical treatments are based on hydrodynamic theories that predict the macroscopic behavior of a system that detonates, such as changes in pressure, temperature, and density (Fickett and Davis 1979; Fickett 1985). These models, however, do not give information about the microscopic chemical and physical processes occurring during this violent event and in many instances, rely on substantial approximation. Very little is known about the chemical reactions that initiate and sustain a detonation, although theoretical (Tsai and Trevino 1984; Tsai 1990; Blais and Stine 1990; Karo, Hardy, and Walker 1978; Elert et al. 1989; Kawakatsu and Ueda 1988, 1989; Kawakatsu, Matsuda, and Ueda 1988; Brenner 1992; Robertson et al. 1992; White et al. 1994; Brenner et al. 1993) and experimental methods (Gupta et al. 1995; Fried and Ruggiero 1994; Dlott and Fayer 1990; Tokmakoff, Fayer, and Dlott 1993; Chen, Tolbert, and Dlott 1994; Chen et al. 1995; Hong, Chen, and Dlott 1995) are being directed toward unraveling details of these ultrafast, violent events.

The method of molecular dynamics is a powerful and well-established simulation technique to provide details of the atomistic processes occurring in a chemical reaction (Raff and Thompson 1985). Though the majority of molecular dynamics simulations have focused on gas-phase problems, computer power has increased to the point that molecular dynamics simulations of condensed phase can be realized. As early as the 1970s, molecular dynamics simulations of simple solid models predicted reasonable features expected from a shocked solid (Holian et al. 1980; Powell and Batteh 1979, 1980). More sophisticated models incorporated energy release reactions that could predict detonation (Tsai and Trevino 1984; Tsai 1990; Brenner 1992; Robertson et al. 1992; White et al. 1994; Brenner et al. 1993); however, the models either described the chemistry that drive the detonation qualitatively incorrectly (Tsai and Trevino 1984;

1

Tsai 1990; Karo, Hardy, and Walker 1978), or the models had undesirable features (Brenner 1992; Robertson et al. 1992; White et al. 1994; Brenner et al. 1993).

It is our intention to use the method of molecular dynamics to investigate the microscopic processes that occur during a detonation and to determine the properties of the system that affect this phenomenon. It is also hoped that relevant mechanisms will be revealed in the process. Before we can do this, we must first develop a model that more correctly describes exothermic chemical reactions, and determine whether it can adequately simulate the phenomenon known as a detonation. We have developed such a model, the features of which are described in the accompanying paper (Rice et al., in press). The focus of the study presented here is to compare our molecular dynamics simulations of a shock-initiated reacting crystal with predictions of classical hydrodynamic theory of detonation. Details and results of the two types of calculations will be presented and a comparison given.

The results of the first calculation, the determination of the equation of state of the system, will be used to evaluate the classical conservation equations that relate the mass, momentum, and energy of the quiescent crystal with the state behind the detonation wave (Fickett and Davis 1979; Fickett 1985). The three conservation equations are:

$$\text{Conservation of Mass:} \quad \rho_0 D = \rho(D-u) \quad (1)$$

where ρ_0 is the density of the undisturbed crystal, ρ is the density of the system behind the shock front, D is the velocity of the wave propagating through the undisturbed crystal (constant for an unsupported detonation), and u is the velocity of the products behind the detonation wave;

$$\text{Conservation of Momentum:} \quad p - p_0 = \rho_0 u D, \quad (2)$$

where p and p_0 are the pressures of the products behind the shock front and quiescent crystal, respectively. The variable u can be eliminated from Equations (1) and (2) resulting in the Rayleigh line

$$R = \rho_0^2 D^2 - (p - p_0)/(v_0 - v) = 0. \quad (3)$$

The final equation requiring conservation of energy is

$$\text{Conservation of Energy:} \quad e + pv + 1/2(D - u)^2 = e_0 + p_0 v_0 + 1/2 D^2, \qquad (4)$$

where e, e_0, and v, v_0 are the specific internal energies and specific volumes of the final and initial states, respectively. The term "specific" as used here with respect to some quantity refers to that quantity normalized to unit mass. The variables D and u can be eliminated from Equation (4) using Equations (1) and (2) to a form that is referred to as the Hugoniot function.

$$h(T,v) = e - e_0 - 1/2(p - p_0)(v_0 - v). \qquad (5)$$

The set of (T, v) for which Equation (5) is zero make up the $h(T_H, v_H)$ curve known as the Hugoniot curve. The intersection of Equations (3) and (5) determine the state of a system (p, v) for a given detonation velocity, D. There are a series of Rayleigh lines, defined by the parameter D, that intersect the Hugoniot curve; all but one give two solutions to Equations (3) and (5) and represent unsteady shocks. The velocity that uniquely satisfies Equations (3) and (5), called the Chapman-Jouguet velocity, corresponds to the $p - v$ point where the Rayleigh line is tangent to the Hugoniot curve. The C-J point is the state of the system corresponding to an unsupported detonation, the event we will attempt to simulate. We will determine the C-J point and detonation velocity for comparison with the molecular dynamics simulation.

The second calculation is the molecular dynamics simulation of a plate impacting the quiescent diatomic molecular crystal, and initiating reaction. This will be denoted throughout as the computer experiment. We will compare the predicted Chapman-Jouguet point and velocity with the shock wave velocity and state of the system from our computer experiment.

This report will first briefly describe the model, the details of the calculations and conclude with results, discussion, and comparison of the two predictions. All calculations described hereafter are two-dimensional.

3

2. MODEL

The interaction potential used to describe the two-dimensional crystal of diatomic molecules arranged in a herringbone lattice is similar to that used by Brenner et al. (1993).

$$V = \sum_{i}^{N} \sum_{j>i}^{i} \left\{ f_c(r_{ij}) \left[\left(2 - \overline{B_{ij}} \right) V_R(r_{ij}) - \overline{B_{ij}} V_A(r_{ij}) \right] + V_{vdW} \right\} \qquad (6)$$

The functions and parameters used in Equation (6) are given in Table 1. The features of this potential energy function are detailed in the accompanying paper (Rice et al., in press). The low temperature, ambient pressure lattice parameters for a unit cell of this crystal in the x and y directions (denoted a and b, respectively) are 4.34 and 6.27 Å. A unit cell is illustrated in the inset of Figure 1. The unit cell contains two molecules; center-of-bond (COB) fractionals are at (0.25, 0.25) and (0.75, 0.75), respectively. The equilibrium A-B bond distance is 1.35 Å, and the angles Θ of the bonds of the two A-B molecules relative to crystal x-axis are ±29.1°.

3. DETAILS OF THE CALCULATIONS

3.1 <u>Cell-Linked Lists</u>. The two types of simulations that we report here require calculating the energy and energy first derivatives of Equation (6). In principal, Equation (6) requires that (N-1) interactions must be calculated for each atom in the N-atom system. However, for a specific atom i, there are only a small number of neighbors j within the interaction range of the potential and therefore are the only ones out of the N-atom system that need to be considered. It is a CPU-consuming task to determine by brute force which of the (N-1) atoms are within the interaction range of atom i. This problem was circumvented by our use of the method of linked-lists, described in detail by Allen and Tildesley (1987). This method efficiently sorts the atoms into indexed bins according to geometric position. Each bin must be no smaller than the cutoff radius of the interaction potential. The scheme ensures that for a specific atom in a bin, only those atoms in the same or nearest-neighbor bins are included in the summation of Equation (6). The distance between atom i and any other atom not in the same or nearest-neighbor bins (and therefore, outside of the interaction range) is not calculated, thus providing considerable CPU savings. For the Monte Carlo simulations (section 3.2), each bin consists of nine unit cells (three in each of the x and y directions). For the molecular dynamics simulations that are used in calculating the equation of state

4

Table 1. Parameters and Functional Forms Used for the Potential Energy Expression in Equation (6)

Parameter	Value	Functional Forms
D_e^{AA} (eV)	5.0	$V_R(r) = \dfrac{D_e}{S-1}\exp\left[-\alpha\sqrt{2S}\,(r-r_e)\right]$
D_e^{BB} (eV)	2.0	
D_e^{AB} (eV)	1.0	$V_A(r) = \dfrac{SD_e}{S-1}\exp\left[-\alpha\left(\dfrac{2}{s}\right)^{\frac{1}{2}}(r-r_e)\right]$
r_e^{AA} (Å)	1.2	
r_e^{BB} (Å)	1.5	
r_e^{AB} (Å)	1.35	$\overline{B}_{ij} = \dfrac{1}{2}\left(B_{ij} + B_{ji}\right)$
S	1.8	
α (Å^{-1})	2.7	$f_c(r_{ij}) = \begin{cases} 1, & r<2.0 \\[2mm] \dfrac{1}{2}[1+\cos(\pi(r-2)], & 2.0\le r\le 3.0 \\[2mm] 0, & 3.0\le r \end{cases}$
G	7.5	
m (Å^{-1})	3.5	
n	0.5	
ε (eV)	0.005	$B_{ij} = \left\{1 + G\displaystyle\sum_{k\neq i,j} f_c(r_{ik})\exp\left[m\left(r_{ij}-r_{ik}\right)\right]\right\}^{-n}$
σ (Å)	2.988	
mass$_A$ (amu)	15.0	
mass$_B$ (amu)	46.0	$V_{vdW} = \begin{cases} 0, & r<1.75 \\[2mm] P_O + r\left[P_1+r\left(P_2+rP_3\right)\right] & 1.75\le r<2.91 \\[2mm] 4\varepsilon\left[\left(\dfrac{\sigma}{r}\right)^{12} - \left(\dfrac{\sigma}{r}\right)^{6}\right] & 2.91\le r<7.31 \\[2mm] \displaystyle\sum_{i=3}^{5} c_i(r-7.32)^i & 7.31\le r<7.32 \\[2mm] 0 & 7.32\le r \end{cases}$
P_O (eV)	0.4854	
P_1 (eV-Å^{-1})	−0.7184	
P_2 (eV-Å^{-2})	0.3455	
P_3 (eV-Å^{-3})	−0.05344	
c_3 (eV-Å^{-3})	925.4631	
c_4 (eV-Å^{-4})	138743.7872	
c_5 (eV-Å^{-5})	5548241.6326	
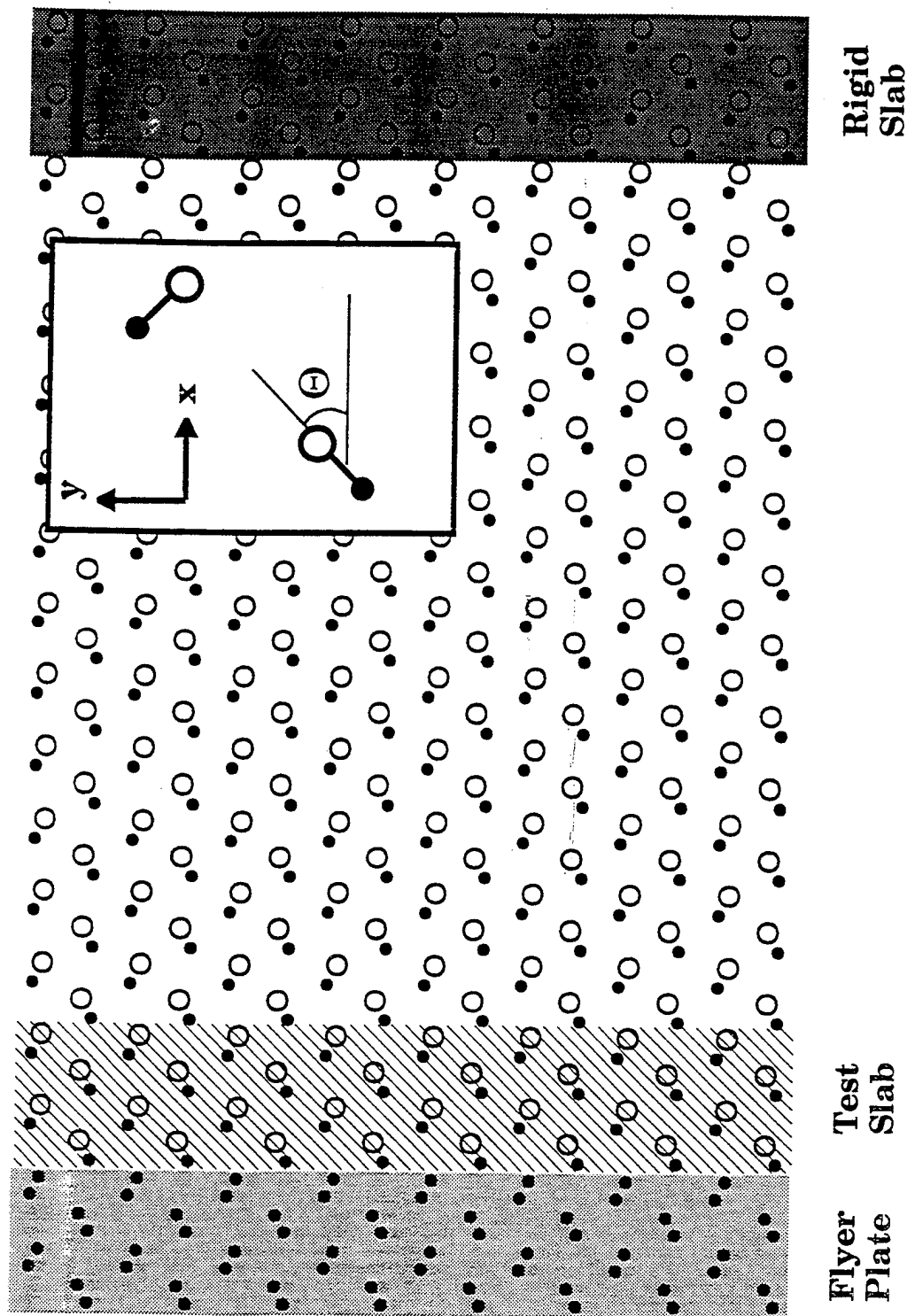
Figure 1. A schematic of the model used in the molecular dynamics simulation of shock-induced reaction. Atom type A (mass = 15 amu) is denoted by filled circles; atom type B (mass = 46 amu) is denoted by open circles. The inset serves to define the geometry of the unit cell. The characteristics of the various shaded zones are discussed in the text. The angle Θ denotes the orientation angle of the molecular bond relative to the crystal x-axis.

(section 3.3), for v/v_0 greater than 0.70, each bin consists of four unit cells (two in each of the x and y directions). For v/v_0 less than 0.70, each bin consists of six unit cells (three in the x direction and two in the y direction). For the molecular dynamics computer experiments in which flyer plate impact initiates the shock wave (section 3.4), each bin consists of four unit cells (two in each of the x and y directions).

3.2 <u>NPT Monte Carlo Simulations</u>. A series of NPT Monte Carlo simulations were performed to determine the low-temperature (20 K), ambient pressure crystal structure and sound speed. We also performed Monte Carlo calculations for pressures up to 0.55 eV/$Å^2$. The results of these calculations were used as starting geometries for our equation-of-state calculations detailed as follows and given in Table 2.

The sound speed of a crystal is proportional to the slope of the p-ρ curve (Fickett and Davis 1979; Fickett 1985); to obtain the sound speed of our low-temperature, ambient pressure crystal, we calculated the density at each pressure in Table 2 and fitted the pressure from 0.015 to 0.0 eV/$Å^2$ to a cubic polynomial in density. The sound speed obtained from the fit is 1.2 km/s for this crystal. We also fitted <a> and <b>, the average lattice constants of the unit cell in the x and y directions, respectively, to quadratics in pressure, to provide initial lattice parameters for the trajectories calculated to determine the equation of state.

The simulation box, with periodic boundary conditions imposed for both dimensions, consisted of nine unit cells in each of the x and y directions. NPT Monte Carlo simulations were symmetry-restricted: In other words, at each attempted step, the atomic positions of all atoms in the system were determined from the positions of the atoms of a single molecule, which we will denote as the target. The geometric parameters sampled in these simulations were the lattice parameters, which determine the volume of the unit cell, and the molecular parameters of the target in the unit cell. The position of the COB of the target molecule was fixed at the lattice fractional (0.25, 0.25), and the bond length and orientation angle of the A-B molecule relative to the crystal x-axis was allowed to be varied through the Monte Carlo sampling. Images of the target had the same molecular geometries as the target, but were translated by the lattice spacings. The COB of the second molecule in the unit cell as the target was fixed at the lattice fractional (0.75, 0.75), and the molecule was assigned the same bond length as the target, but had the negative value of the orientation angle of the target sampled through Monte Carlo. This ensured the herringbone lattice structure.

Table 2. Lattice Parameters, Density, and Molecular Geometry vs. Pressure

Pressure (eV/Å^2)	$<a>$ (Å)	$<b>$ (Å)	$<\rho>$ (amu/Å^2)	$<r_{ij}>$ (Å)	$<\theta_{ij}>$ (°)
0.0	4.34	6.27	4.4836	1.349	29.1
0.00005	4.33	6.28	4.4869	1.349	29.3
0.0001	4.33	6.27	4.4936	1.349	29.1
0.0005	4.32	6.25	4.5185	1.349	29.1
0.001	4.31	6.22	4.5505	1.349	29.0
0.0025	4.24	6.19	4.6476	1.349	29.8
0.0125	4.13	5.94	4.9735	1.347	29.0
0.015	4.11	5.90	5.0309	1.346	29.0
0.05	3.98	5.67	5.4054	1.340	29.3
0.10	3.85	5.46	5.8040	1.332	28.6
0.15	3.76	5.33	6.0878	1.326	29.1
0.20	3.71	5.23	6.2887	1.321	28.8
0.25	3.67	5.14	6.4687	1.317	28.6
0.30	3.63	5.08	6.6161	1.314	28.6
0.35	3.59	5.02	6.7703	1.311	28.5
0.40	3.56	4.96	6.9083	1.310	28.3
0.45	3.53	4.91	7.0398	1.310	28.1
0.50	3.50	4.85	7.1849	1.312	27.9
0.55	3.46	4.77	7.3939	1.317	27.5

Several Monte Carlo calculations were performed using different initial configurations to see if the results converged to the same value, regardless of initial state. The molecular geometry and lattice spacings for the crystal were initially set to values that were far (up to ±33%) from equilibrium values. For example, the initial bond length of the target ranged from 1.0 to 1.8 Å, and the lattice spacings were either 0.8 Å larger or smaller than equilibrium values. A total of 1,000 Markov steps were attempted, during which time the system relaxed to near its thermal equilibrium configuration. At this point, 4,000

points were used in the averaging of the results. Once the lattice parameters were obtained, we determined the equilibrium orientation of the molecules in the crystal corresponding to those lattice parameters using the Newton-Raphson energy minimization method (Press et al. 1986).

3.3 <u>Molecular Dynamics Simulations: Equation-of-State Calculations</u>. In order to calculate the Hugoniot function in Equation (5), we are required to calculate the equation of state of the system behind the shock front. Additionally, we need to know the state of the quiescent system. We have used molecular dynamics to determine these states, in the manner outlined by Erpenbeck (1992). In that study, Erpenbeck determined the equation of state and Hugoniot curve for a simple diatomic fluid using thermodynamic averages calculated from molecular dynamics trajectory ensembles. The initial conditions for each trajectory in the ensembles were selected using standard Metropolis Monte Carlo sampling. We have followed the procedure outlined in Erpenbeck (1992), except rather than use ensembles of short-lived trajectories for our averaging, we extracted time-averaged thermodynamic properties from a single long-lived trajectory for a given set of initial conditions. Each trajectory was integrated until the averages of the thermodynamic properties converged. Most averages converged within 5 ps; some trajectories were integrated up to 10 ps before convergence was met. Thermodynamic properties were calculated for v ranging from 0.123 to 0.223 Å^2/amu. We also differed in the way we calculated the pressure of the system; Erpenbeck used the virial function to calculate his pressures (Erpenbeck 1992); we followed the method outlined in Tsai (1979). Periodic boundary conditions were imposed in both x and y directions. The initial conditions of the crystal for a simulation corresponding to each v were determined from the quadratic fits of the lattice parameters given in Table 2. The molecular bond length and orientation of the molecular bond relative to the crystal x-axis were set to 1.35 Å and 29°, respectively. Kinetic energy ranging from 2,000 K to 15,000 K was equipartitioned among the atomic momenta components. The equations of motion of the system were then integrated for approximately 6.5 ps. The final conditions of the warmup trajectory were then used as the initial condition for the trajectory from which the thermodynamic averages would be extracted. This final trajectory was integrated until the thermodynamic averages converged.

Hamilton's equations of motion for this system were integrated using an Adams-Moulton fourth-order predictor-corrector (Miller and George 1972) integrator with error tolerance set to 10^{-5}. We found that the results using this tolerance did not deviate from those in which the tolerance was set much smaller. Energy conservation was monitored, and accuracy to 0.0003 eV was obtained.

3.4 Molecular Dynamics Simulations: Computer Experiment of a Detonation. We utilized a method developed by Tsai and Trevino (1981) in which the simulation box expands into the undisturbed region as the shock wave passes throughout the crystal. We are interested only in the region immediately preceding and following the shock front. To simulate an infinitely large crystal several microns from the shock front would merely increase the simulation time, without increasing our knowledge of the phenomenon of interest, namely the detonation and the region affected by it. Therefore, we implemented the following scheme: The simulation box initially consists of A-B molecules at the equilibrium position. It is a 16 × 8 area of unit cells, with periodic boundary conditions imposed in the y direction only. Figure 1 illustrates the initial state of the simulation system. For discussion purposes throughout this report, we will denote a fragment of the molecular crystal consisting of 2 × 8 unit cells as a "slab." To minimize surface effects at the far right edge of the cell (which is furtherest from shock impact of the plate), we held a slab of A-B molecules rigid throughout the simulation, with the molecules fixed in their equilibrium orientation. All other A-B molecules and flyer plate atoms are allowed to move according to the equations of motion. The flyer plate is a slab of A-A molecules (located at the far left of Figure 1), chosen because of their stability in order that chemical reactivity would not contribute to the mechanical energy that is transferred to the stationary A-B molecular crystal upon impact. Note that a slab in this figure is highlighted and designated as "test slab." The average kinetic energy for the atoms in the test slab is calculated at each integration step. If this value exceeds 15 K, then a new slab of A-B molecules is inserted between the rigid slab and the far right edge of the slab of atoms that are allowed to move throughout the simulation. The molecules in the new slab are initially at their equilibrium position, and kinetic energy corresponding to 20 K is partitioned between the x- and y-momentum components for each atom. When a new slab of molecules is added, the test slab is shifted by one slab length to the right. In this scheme, the length of the undisturbed crystal is constant and consists of seven slabs of quiescent A-B molecules (not including the rigid slab). We found that the energy rapidly equilibrated in this region and was partitioned equally into potential and kinetic energy (average kinetic energy in this region is 10 K). This latter observation serves as ad hoc justification for the treatment of the undisturbed region.

Initial conditions were selected as follows: All atoms in the simulation box are at the equilibrium position; the A-A molecules in the flyer plate have the same lattice parameters and orientational angles as the A-B molecules; the only difference in crystal structure between the flyer plate and quiescent A-B crystal is the molecular size of the molecules. Each atom is given kinetic energy totaling 20 K, partitioned between the x- and y-momentum components. A short warmup trajectory is integrated for 0.7 ps, to allow randomization of the energy in the crystal. Because the flyer-plate slab of A-A molecules is not in the

equilibrium position (it has smaller molecular bond distances than molecules in the A-B crystal), some heat will be released into the system during this warmup trajectory as the A-A atoms relax toward the equilibrium position for those lattice parameters. We found through monitoring the average kinetic energy of the A-A molecules in the flyer plate and of the A-B molecules in the adjacent slab during the warmup trajectory that the amount of heat released is insignificant. The average kinetic energy of the molecules in both slabs fluctuated about 10 K throughout the warmup trajectory. After the warmup trajectory, the flyer plate atoms are given impact velocities in the positive x-direction. As the equations of motion of the system are integrated, the flyer plate atoms strike the quiescent A-B molecular crystal. We found that for this size of flyer plate (one slab), the minimum velocity of the flyer plate to initiate an unsupported detonation is 4.7 km/s. Anything below this velocity caused a few reactions at the initial impact, but apparently were not enough to sustain the detonation.

Energy conservation was monitored, and accuracy to 0.0003 eV was obtained until a new slab of atoms was added. At this point, there is a discontinuity in the energy of the system (more equations of motion are being integrated due to the addition of atoms), but energy is conserved until another slab is added during the simulation.

The mass density, kinetic temperature, and two-dimensional pressures in the steady region of the reactive flow in our simulations were calculated in a manner outlined in Tsai and Trevino (1981). Our simulations differ from the piston-driven shock wave results calculated by Tsai and Trevino (1981) in that our simulations result in unsupported detonations. An unsupported detonation has a following flow behind the steady reaction zone that changes with time, and the conservation equations [Equations (1)–(5)] cannot be applied to this region (Fickett and Davis 1979; Fickett 1985). Therefore, we had to make some approximations in calculating kinetic temperature and two-dimensional pressures in the rarefaction zone. To calculate the kinetic temperature associated with thermal motion for regions throughout the crystal, we had to remove the kinetic energy associated with mass flow velocity for the region. For areas within the steady reaction zone, the local mass flow can be determined from Equation (1). For areas in the rarefaction zone, we approximated the local flow velocity to be the center of mass velocity of all of the particles within this area.

Equation (2) can be employed to calculate the pressure through the shock front for the steady portion of the shock wave. In the rarefaction region, Equation (2) no longer applies. Instead, the instantaneous

11

stress is obtained by the method outlined in Tsai (1979), which uses the forces and momentum flux that intercept lines moving at the local flow velocity.

4. RESULTS

4.1 Equation-of-State Calculations.   We have calculated, using molecular dynamics, the thermodynamic properties of the quiescent A-B molecular crystal and the sample at specific volumes from 0.123 to 0.188 Å^2/amu and for temperatures ranging from approximately 2,000 K up to 10,000 K. The results are shown in Table 3. Figures 2 and 3 show the temperature dependence of both the Hugoniot function [Equation (5)] and pressure for various specific volumes. The symbols represent the results of the molecular dynamics averages of these properties, and the curves in Figure 3 are fits of the pressure to quadratic polynomials in temperature.   The quadratic fits of Equation (5) to temperature were not illustrated in Figure 2, for clarity of the figure. The Hugoniot temperatures (T_H), the temperature at which Equation (5) is zero for each specific volume, were extrapolated from the quadratic fits of Equation (5) to temperature, and are listed in Table 4. The corresponding Hugoniot pressure, P_H, was calculated at the T_H for each specific volume using the quadratic fit of pressure to temperature, and are also listed in Table 4. These values can be used in Equation (3) to determine detonation velocities, D, as functions of specific volume. The detonation velocities corresponding to each T_H and P_H are given in Table 4 and shown as a function of specific volume in Figure 4.   The Chapman-Jouguet velocity is the minimum detonation velocity corresponding to the set of Hugoniot pressures and specific volumes. The curve shown in Figure 4 is a fit of the detonation velocities to a quadratic polynomial in specific volume. The position of the minimum of D, calculated using the quadratic polynomial fit shown in Figure 4, corresponds to a specific volume of 0.141 Å^2/amu (or density of 7.09 amu/Å^2). The detonation velocity at this density is 0.717 Å/t.u. (7.0 km/s).

Figure 5 shows the Hugoniot curve and the Rayleigh line that uses the Chapman-Jouguet detonation velocity determined from the polynomial fit shown in Figure 4.   Indeed the curves intersect at the C-J point. The C-J pressure is 0.86 eV/Å^2.

4.2 Molecular Dynamics Simulation of Detonation.   Molecular dynamics simulations of a flyer plate impacting a quiescent crystal were performed with six impact velocities ranging from 4.6 km/s to 12 km/s. The simulations will be denoted hereafter by the impact velocity of the flyer plate. The position of the shock wave as a function of time for each of these six simulations are illustrated in Figure 6.   The

12

Table 3. Thermodynamic Properties vs. Specific Volume

| v ($Å^2$/amu)	T (K)	e (eV/amu)	P (eV/$Å^2$)
0.223048	10	−0.016945	0.000790
0.187541	7,702	−0.005269	0.468962
	8,541	0.000381	0.483094
	9,116	0.006033	0.478626
	10,076	0.011683	0.484239
0.167262	6,671	−0.003577	0.623313
	7,302	0.002074	0.625804
	8,303	0.007724	0.618631
	8,845	0.013375	0.617379
0.155948	4,247	−0.007119	0.648500
	5,763	−0.001468	0.707511
	5,836	−0.001468	0.721500
	6,491	0.004183	0.705964
	6,607	0.004183	0.725363
	7,197	0.009833	0.703152
	7,444	0.009832	0.697245
	8,113	0.015484	0.681139
	8,253	0.015484	0.716467
0.147425	4,215	−0.004544	0.756504
	5,026	0.001107	0.778300
	5,791	0.006758	0.753580
	6,923	0.012409	0.797745
	7,689	0.018059	0.786444
0.138170	3,699	−0.001146	0.871516
	4,645	0.005070	0.862671
	5,311	0.010720	0.846950
	6,531	0.016370	0.889304
	7,386	0.022021	0.879788
0.127342	2,608	0.002651	0.919353
	3,108	0.005477	0.922500
	3,962	0.011127	0.900155
	4,806	0.016778	0.906584
	5,816	0.022429	0.931453
	6,999	0.028079	0.983333
0.123003	2,876	0.008239	0.918458
	3,704	0.013890	0.941040
	4,661	0.019540	0.942793
	5,672	0.025191	0.971843
	6,927	0.030842	1.021582
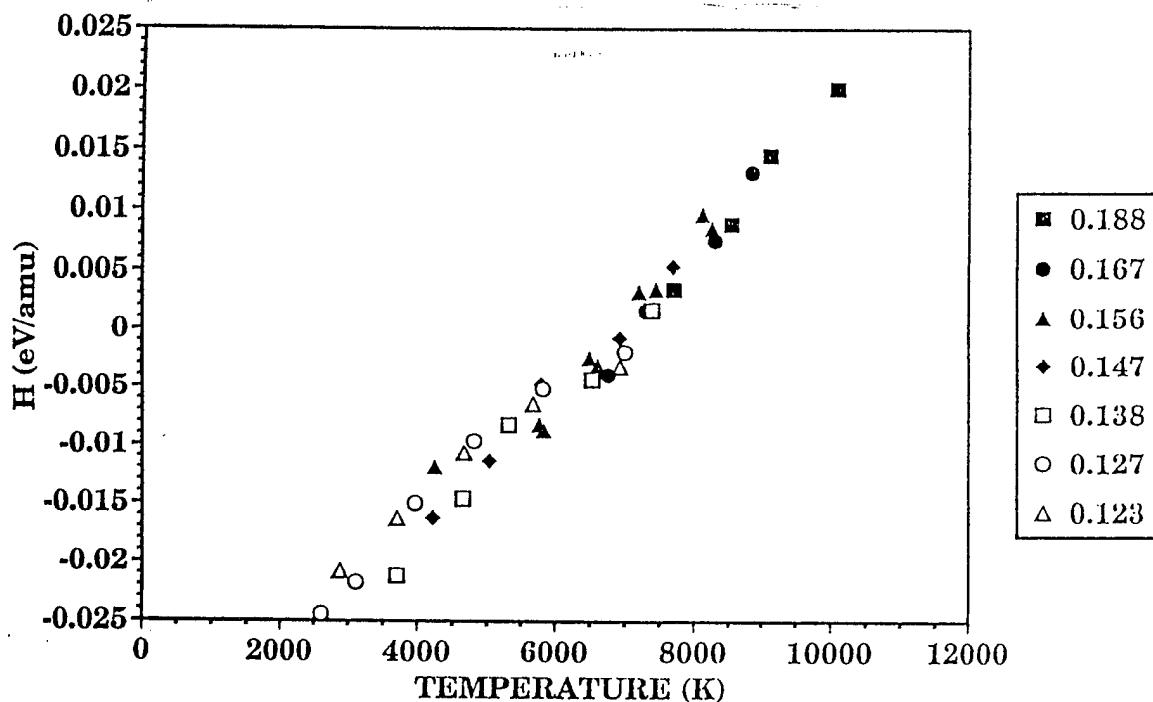
Figure 2. Hugoniot function (Equation 5) vs. temperature for various specific volumes, values of which are denoted in the legend. These are obtained from the results of molecular dynamics equation-of-state calculations.
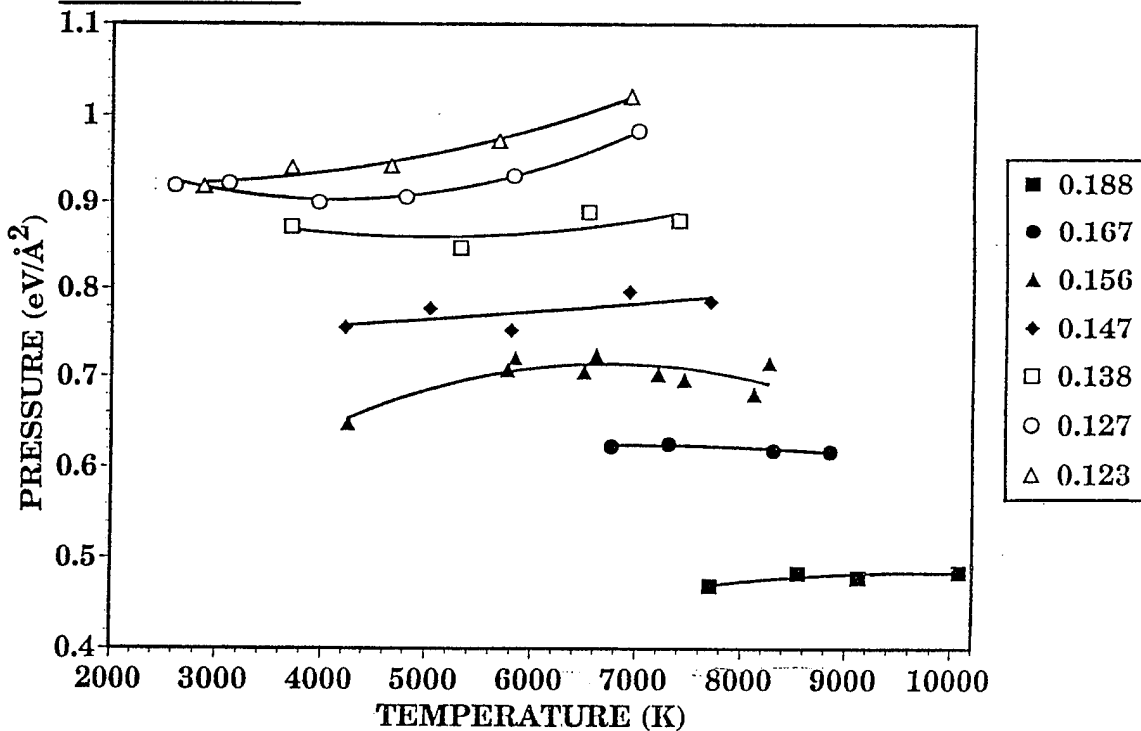

Figure 3. Pressure vs. temperature for various specific volumes, values of which are denoted in the legend. These are the results of molecular dynamics equation-of-state calculations. The solid lines denote quadratic fits in temperature.

14

Table 4. Hugoniot Temperatures, Pressures, and Detonation Velocities vs. Specific Volume

v (Å^2/amu)	T_H (K)	P_H (eV/Å^2)	D (Å/t.u.)[a]
0.187541	7,335	0.46463	0.806168
0.167262	7,235	0.62413	0.745588
0.155948	7,063	0.71394	0.727154
0.147425	6,834	0.78271	0.717220
0.138170	7,125	0.88206	0.718711
0.127342	7,500	1.01308	0.725406
0.123003	8,051	1.07319	0.730263

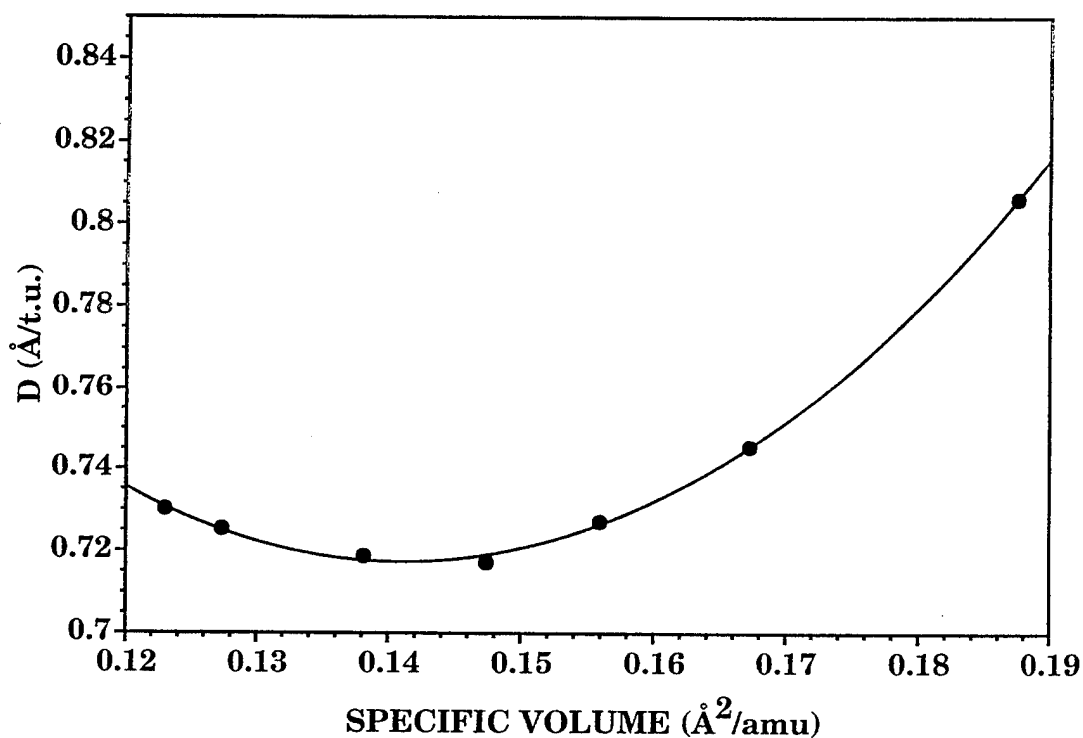[a] 1 t.u. = 1.018066×10^{-14} s.

Figure 4. Detonation velocity D as a function of specific volume obtained from the Hugoniot temperatures and pressures at each specific volume (see Equation 2). The solid curve denotes a quadratic fit in specific volume. One t.u. equals 1.018066×10^{-14} s.
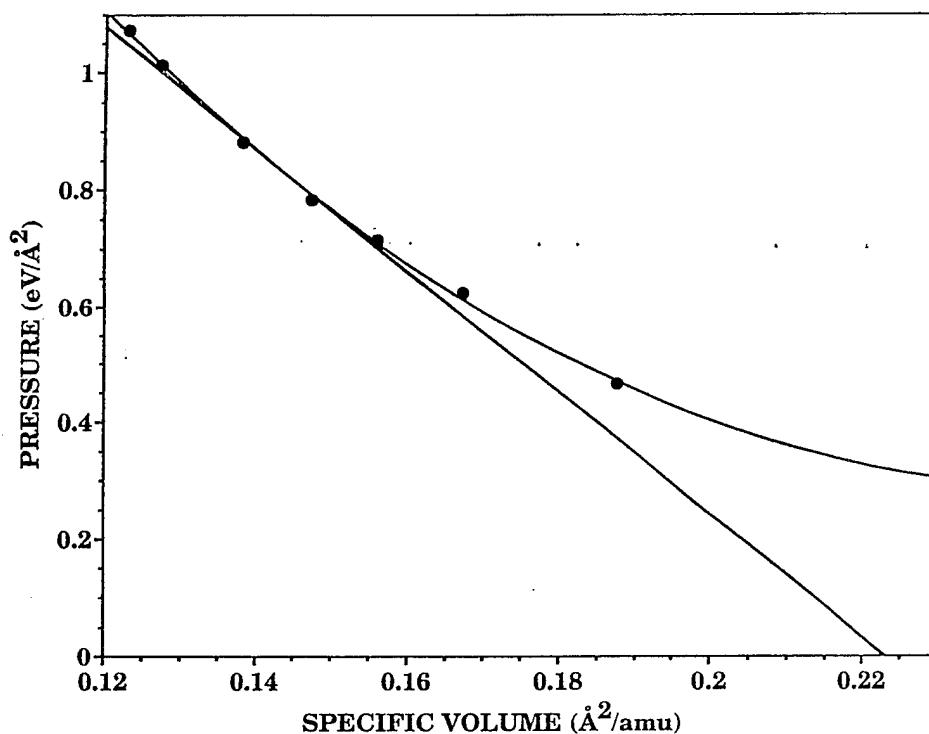
15

Figure 5. Hugoniot pressure vs. specific volume obtained from the results of molecular dynamics equation-of-state calculations. The straight line tangent to the Hugoniot curve is the Rayleigh line corresponding to the Chapman-Jouguet condition. The slope of this line is consistent with the Chapman-Jouguet velocity determined from the data shown in Figure 4.
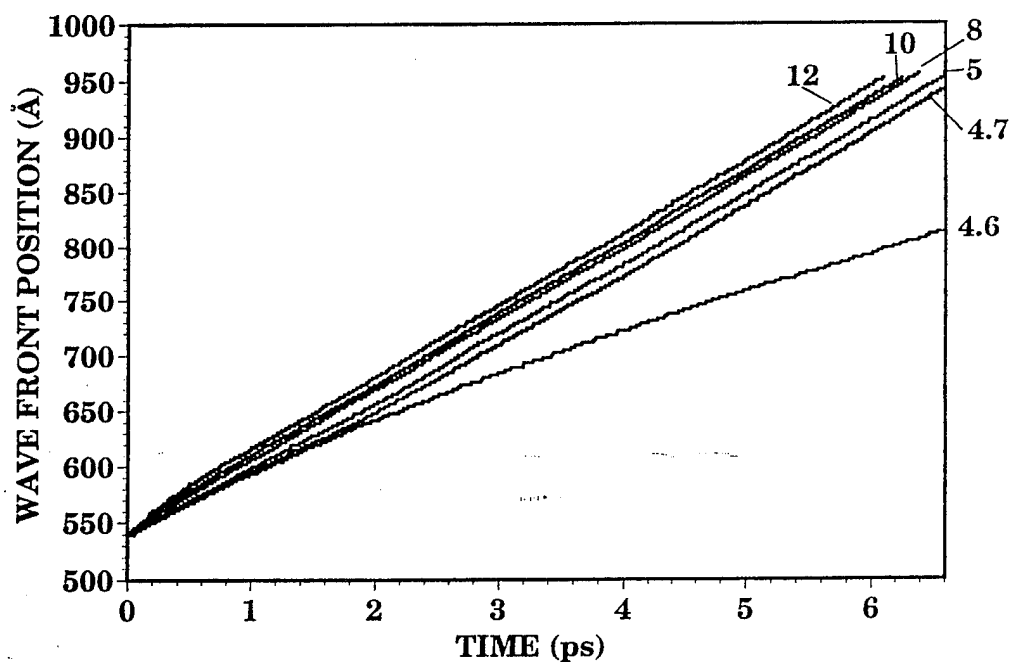

Figure 6. Position of the shock front as a function of time for the six molecular dynamics simulations. The numbers denote the velocities of the flyer plate in kilometers per seconds.

16

threshold for initiation of detonation for this plate thickness is found to be 4.7 km/s; detonation was not sustained for plate impacts smaller than this. With the exception of the 4.6 km/s simulation, the slopes of the shock fronts are the same by 3.5 ps into each simulation. Before this time, the slopes differ as the detonations reach steady state. The steady-state detonation velocity is 6.6 km/s. The faster the impact velocity, the sooner the detonation reaches steady state. The shock wave initiated with flyer plate impact of 12 km/s reaches the steady-state detonation velocity within 0.1 ps. The detonation velocity determined through these computer experiments is 6.1% smaller than the C-J detonation velocity predicted from hydrodynamic theory (see section 4.1).

Thermodynamic property profiles for the computer experiments have similar features. A typical snapshot of the system for the 12 km/s simulation at 7.8 ps is shown in Figure 7; thermodynamic property and species profiles corresponding to this time are shown in Figure 8. Figure 7 shows three distinct regions: Undisturbed crystal, the reaction zone, in which the molecules are compressed and are undergoing reaction, and the rarefaction region, which consists of vibrationally-excited homonuclear products. We have defined the reaction zone as the area between the position of the shock front and the point (along the x-axis) at which the number of reacted molecules (dissociated from original molecular partner) exceeds the number of unreacted A-B molecules. The point at which the number of reactions exceeds the number of unreacted atoms is illustrated in Figure 8(d); it is approximately 14 Å behind the shock front in this snapshot. We have found that the size of the reaction zone is steady in time, and is on average 14 Å in width. This is illustrated in Figure 9, which shows the width of the reaction zone throughout the 12 km/s simulation. Additionally, the composition and properties of this zone are steady in time. The thermodynamic properties in this region are those we wish to compare with the hydrodynamic predictions. We have calculated the thermodynamic properties of a thin area of the sample directly behind the shock front over the life of the 12 km/s trajectory. This area has the same dimensions of a "slab" as defined in section 3.4. Figures 10(a–c) show the density, pressure, and kinetic temperature of this region over time. The properties are well behaved and steady. The average temperature, pressure and density of this region are: 7,435 K, 0.88 eV/Å^2, and 7.13 amu/Å^2. The average pressure and specific volume of these regions differ by 2.6% and 0.6%, respectively, from the hydrodynamic predictions of the C-J values. The agreement between the two theories is good.

The differences in the results of the two calculations, although small, can be attributed to differences in state composition. In the equation-of-state calculations, an equimolar mixture of A and B atoms was used. In the detonation simulations, however, the number density of B atoms in the slab behind the shock

17

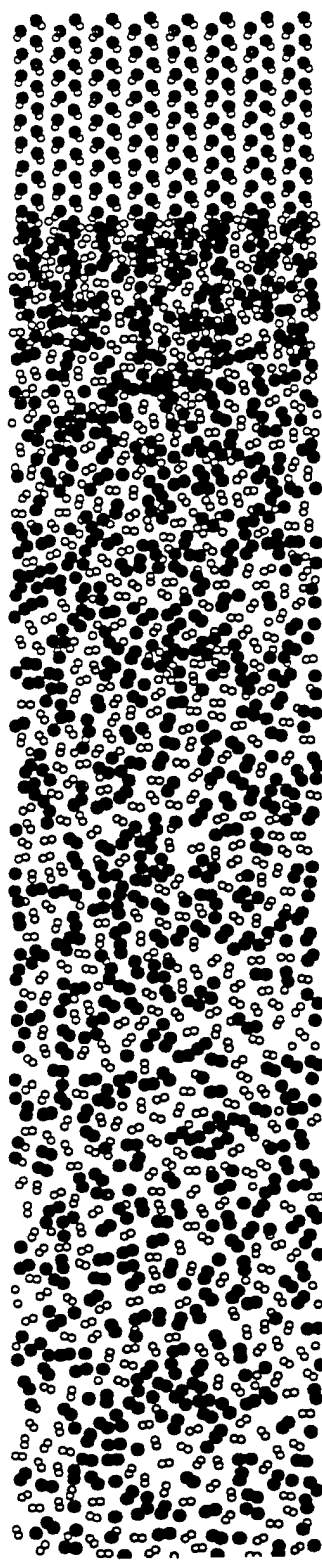Figure 7. A snapshot of the system for the 12 km/s flyer-plate impact at 7.8 ps into the simulation. The dimensions of the sample shown in the snapshot are 300 × 50 Å.
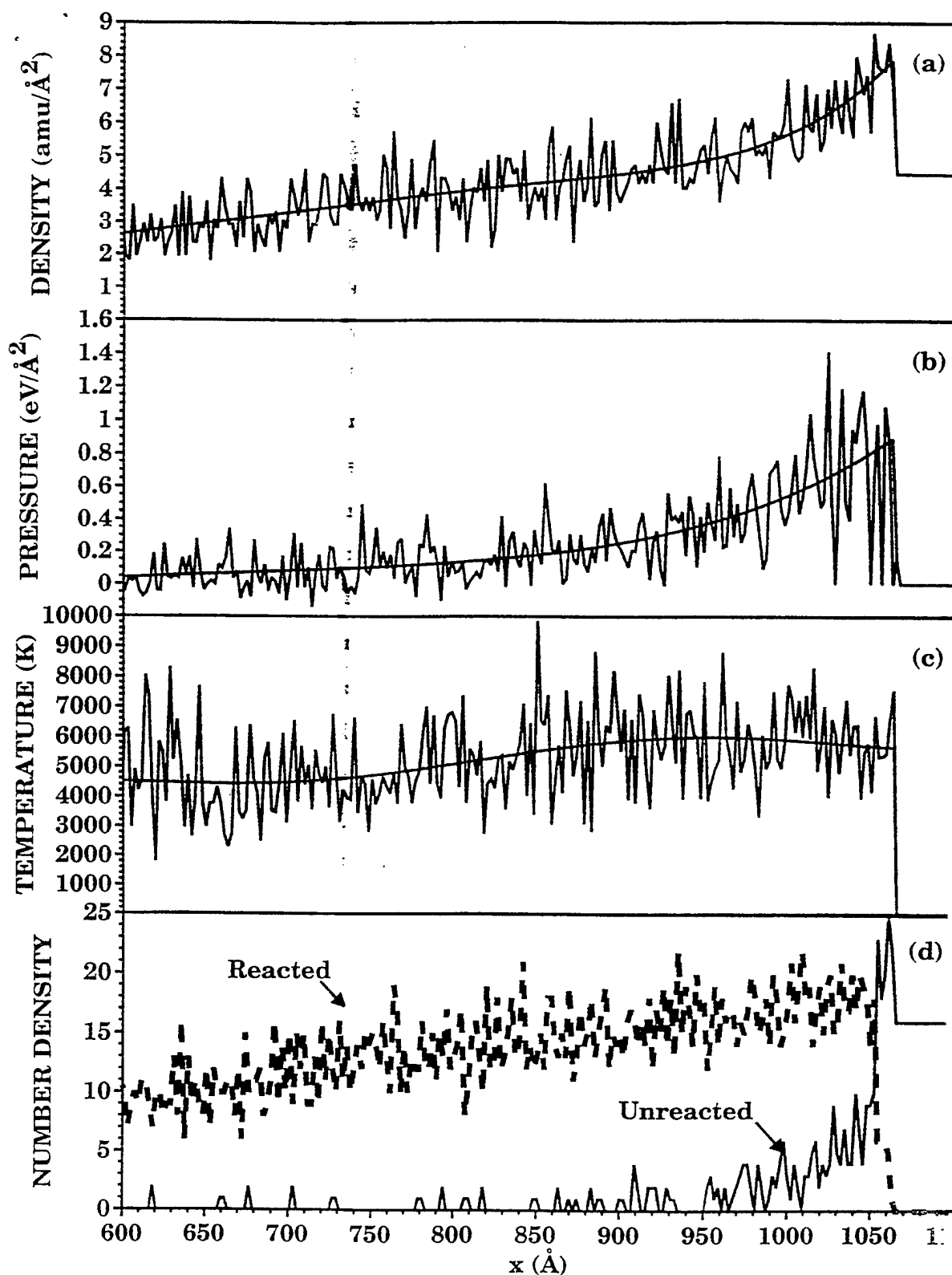
18

Figure 8. Thermodynamic property profiles of the system corresponding to the conditions described in Figure 7. Solid and dashed curves in (d) denote unreacted and reacted A-B molecules, respectively. The smooth curves in (a)–(c) are guides to the eye.
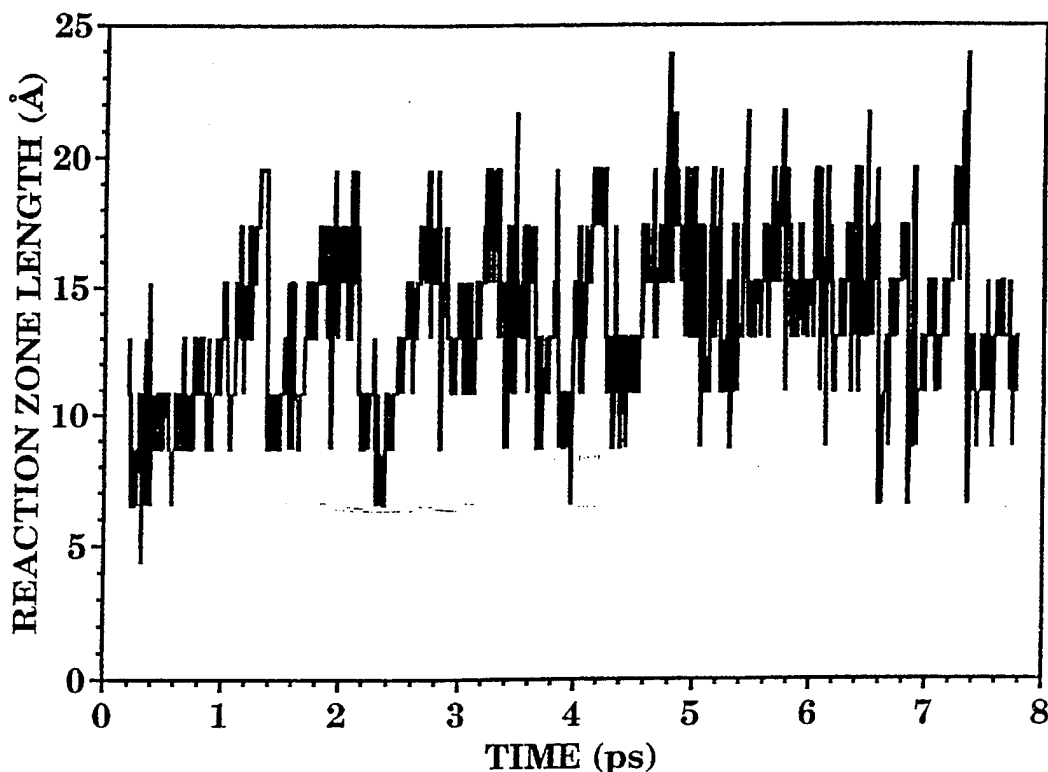
19

Figure 9. <u>Reaction zone length as a function of time through the 12 km/s simulation.</u>

front was consistently higher than the number density of A atoms. The mixture behind the shock front consists, on average, of 57% B atoms, 43% A atoms. Therefore, although the C-J density agrees well with the density behind the shock front in the computer experiment, the chemical composition between the two situations differs. The larger percentage of the heavier B atoms in the detonation simulation is consistent with a detonation velocity lower than the C-J detonation velocity predicted from the results of the equation-of-state calculations.

The zone behind the reaction zone (the rarefaction zone) is unsteady; its properties change with time. The configuration of the system produced in our computer experiments appears to be representative of an unsupported detonation as described in Fickett and Davis (1979) and Fickett (1985), and is almost described by the simplest theory (Fickett and Davis 1979; Fickett 1985). The flow appears to be one-dimensional, the detonation front is almost a jump discontinuity, and the material emerging from the front (the reaction zone) is independent of time. Additionally, the model used in these computer experiments provides almost instantaneous reaction, with only slightly more than 14 Å between the shock front and complete reaction. These properties, as well as the good agreement with the hydrodynamic
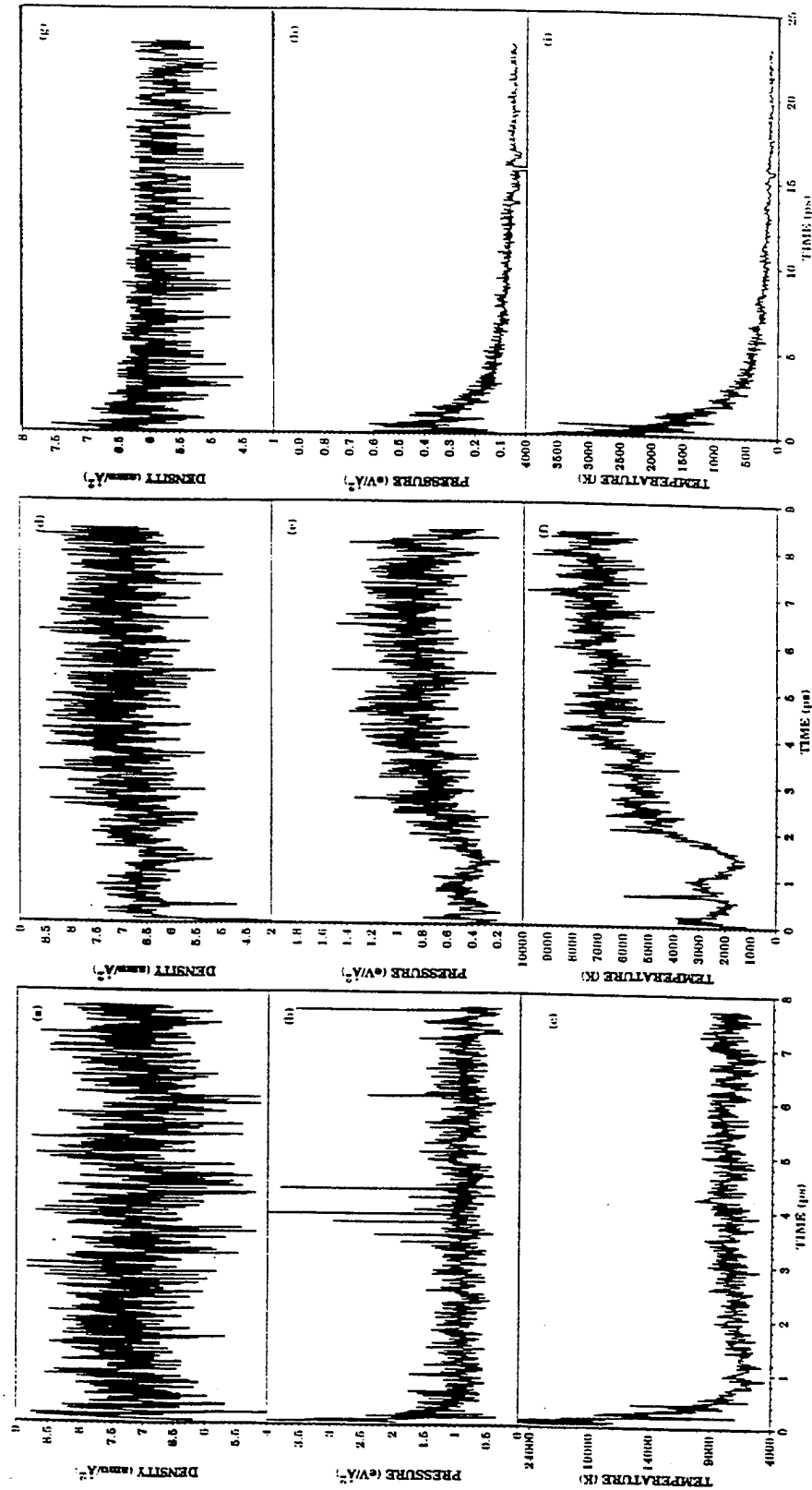
20

Figure 10. Densities, pressures, and temperatures as functions of time for simulations with flyer-plate velocities of 12 km/s (a)–(c), 4.7 km/s (d)–(e), and 4.6 km/s (g)–(i). Note the significant differences in the temperature scales.

21

predictions, indicate that both the method of molecular dynamics and our model of an energetic crystal can reasonably describe the phenomenon of detonation.

We have also calculated the time dependence of the thermodynamic properties of a slab of material (as defined in section 3.4) immediately behind the shock fronts in the computer experiments for plate impacts of 4.7 and 4.6 km/s. The thermodynamic properties behind the shock fronts for these two simulations were evaluated as for the 12 km/s simulation [see Figures 10(d–i)]. The 4.6 km/s system reaches a maximum kinetic temperature, pressure and density of 3,800 K, 0.61 eV/Å^2 and 7.6 amu/Å^2, respectively, within 1 ps into the simulation, but these values are not maintained and rapidly drop to significantly lower values as the simulation progresses. The maximum pressure reached in this experiment is well below the Chapman-Jouguet pressure, although the C-J density is reached (but not maintained) during this trajectory. The profiles for the 4.7 km/s simulation are very similar to those of the 4.6 km/s simulation for the first two picoseconds; however, the thermodynamic properties approach the steady-state detonation averages after this time.

It is worthwhile to examine more closely the differences in the profiles between the simulations of the 4.6 km/s and 4.7 km/s flyer-plate simulations since the former does not lead to sustained detonation and the latter does. Figure 11 shows the densities, pressures, and temperatures of the reaction zone as functions of time during the first two picoseconds of both the 4.6 km/s and 4.7 km/s simulations. The main differences in these properties for the two simulations occur between 0.6–1.0 ps, and then after 1.5 ps. At 0.7 ps, there is a sharp increase in the kinetic temperature for the 4.7 km/s simulation that does not occur for the 4.6 km/s simulation. The temperature then fluctuates near 3,000 K for 0.3 ps in the 4.7 km/s simulation, whereas the temperature for the 4.6 km/s simulation falls below 2,000 K during this same time. The pressure in the 4.7 km/s simulation averages approximately 0.55 eV/Å^2 during this time, whereas the pressure of the 4.6 km/s simulation falls to half that value. Finally, the density of the 4.7 km/s simulation from 0.6 ps to 1.0 ps fluctuates near the C-J value, but the density for the 4.6 km/s simulation during this time period is well below the C-J value.

The two simulations predict similar behavior in properties from 1.0 ps to 1.5 ps, but then the curves diverge. All curves corresponding to the 4.6 km/s simulation decrease monotonically. For the 4.7 km/s simulation, the C-J density is reached and subsequently maintained at 1.6 ps, well before the C-J pressure is reached 0.6 ps later. The temperature for the 4.7 km/s simulation does not reach a steady value until 6 ps into the trajectory; it monotonically increases to 5,500 K at approximately 2.2 ps, and fluctuates about
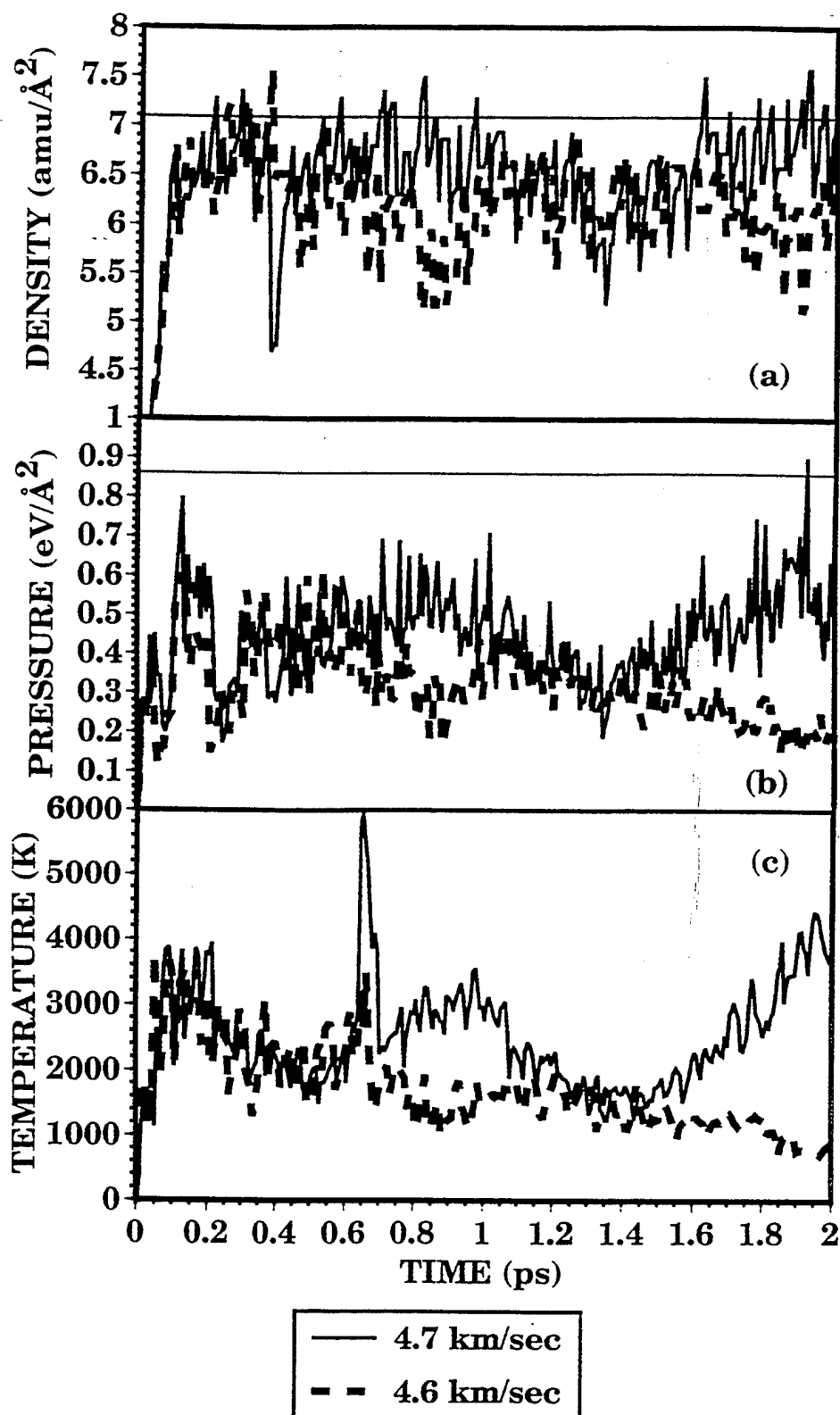
22

Figure 11. A comparison of (a) density, (b) pressure, and (c) temperature as functions of time for the two conditions of flyer-plate velocity which bracket the threshold for sustained unsupported detonation. The straight lines in the density and pressure figures denote the C-J values for these quantities.

this value for approximately 2 ps. It then increases to 6,500 K for another 2 ps, at which point it appears to increase to 7,200 K, about which it fluctuates for the remainder of the trajectory. These fluctuations throughout the simulations, particularly at the beginning, are suggestive of a system sampling a critical region of phase space separating two distinctly different results: namely, sustained, unsupported detonation vs. nonreactive shock. From these results, it would appear that attainment of the C-J density from shock impact is the determining factor for the sustenance of a detonation.

5. CONCLUSIONS

We have presented a comparative study of molecular dynamics computer experiments of an unsupported detonation to hydrodynamic predictions based on the classical conservation equations that relate mass, momentum, and energy of the quiescent crystal with the state behind the detonation wave (Fickett and Davis 1979; Fickett 1985). We calculated the equation of state of the system, through molecular dynamics, in order to evaluate the classical conservation equations and generate the Hugoniot curve for this system. The model used in both the equation-of-state calculations and in the computer experiments describes a reactive crystal consisting of heteronuclear diatomic molecules that release heat upon formation of the homonuclear diatomic products. All calculations presented herein are two-dimensional.

The equation of state of an equimolar mixture of A and B atoms is determined from thermodynamic averages obtained through molecular dynamics simulations for specific volumes ranging from v_0, the low-pressure reduced volume, to $0.55\ v_0$. Equilibrium temperatures and pressures were determined for each reduced volume, and the Hugoniot curve was produced. The Chapman-Jouguet state was then determined; the C-J detonation velocity, density, and pressure are predicted to be 7.0 km/s, 7.09 amu/$\mathring{A}^2$, and 0.86 eV/$\mathring{A}^2$, respectively.

The computer experiments simulate shock-initiated (through flyer-plate impact) reactions in a model energetic crystal. For plate impacts with velocities no less than 4.7 km/s, the shock front and reaction zone propagate through the crystal at a steady rate of 6.6 km/s. The thermodynamic properties and width of the reaction zone are time-independent. The average width of the reaction zone is 14 $\mathring{A}$; this width is the same for all plate impact velocities no less than 4.7 km/s. Time-averaged density, pressure, and temperature immediately behind the shock front in the reaction zone are 7.13 amu/$\mathring{A}^2$, 0.88 eV/$\mathring{A}^2$, and

24

7,435 K, respectively. The following flow is time-dependent; the properties and width of this region change as the simulations progress in time.

Agreement between the computer experiment and the hydrodynamic predictions is good. The largest discrepancy is a 6% difference in the detonation velocities, which we attribute to differences in the chemical composition of the system used in the equation-of-state calculation and that of the reaction zone behind the shock front in the computer experiments. The equation-of-state calculations had an equimolar distribution of A and B atoms in the system, but the state behind the shock front in the computer experiment had, on average, a larger number density of B atoms (57% of the total number) than A atoms (43% of the total number) over the lifetime of the simulation. The larger concentration of the heavier B atoms in the computer experiment could explain the smaller detonation velocity observed in the computer experiments. The C-J pressure and density are in remarkably good agreement with the computer simulations (within 2.5%) even though the chemical composition behind the shock front in the computer experiment differs from that used in the equation-of-state calculations.

Thermodynamic properties of thin regions immediately behind the shock fronts were monitored in time for computer experiments in which flyer plates strike the quiescent molecular crystal with velocities of 4.6 km/s and 4.7 km/s, respectively. Detonation is not sustained for the 4.6 km/s impact; an unsupported detonation results from the 4.7 km/s impact. For the first 1.5 ps of both simulations, the thermodynamic properties have similar values. After this time, the behavior of the properties of the two simulations diverge. All properties corresponding to the simulation with 4.6 km/s flyer-plate impact decrease monotonically after 1.5 ps. At 1.6 ps, the density of the system corresponding to the 4.7 km/s flyer-plate impact reaches and maintains the C-J value. The pressure for the 4.7 km/s simulation subsequently increases monotonically to the C-J value only after the C-J density is attained, suggesting that if the C-J density is reached, then a detonation will be sustained.

These results show that the method of molecular dynamics and our model of a reactive energetic molecular crystal can be used to reasonably simulate the phenomenon of detonation.

25

INTENTIONALLY LEFT BLANK.

6. REFERENCES

Allen, M. P., and D. J. Tildesley. <u>Computer Simulation of Liquids.</u> Oxford: Oxford University Press, and references therein, 1987.

Berthelot, M., and P. Vielle. <u>C. R. Hebd. Sceances Acad. Sci.,</u> vol. 93, no. 18, 1881.

Berthelot, M., and P. Vielle. <u>C. R. Hebd. Sceances Acad. Sci.,</u> vol. 94, no. 149, 1882a.

Berthelot, M., and P. Vielle. <u>C. R. Hebd. Sceances Acad. Sci.,</u> vol. 94, no. 882, 1882b.

Blais, N. C., and J. R. Stine. <u>Journal of Chemical Physics,</u> vol. 93, no. 7914, 1990.

Brenner, D. W. <u>Shock Compression of Condensed Matter,</u> Elsevier Science Publishers B. V.: S. C. Schmidt, R. D. Dick, J. W. Forbes, and D. G. Tasker (eds.), pp. 115, 1992.

Brenner, D. W., D. H. Robertson, M. L. Elert, and C. T. White. <u>Physical Review Letters,</u> vol. 70, no. 2174, 1993.

Chen, S., X. Hong, J. R. Hill, and D. D. Dlott. <u>Journal of Physical Chemistry,</u> vol. 99, no. 4525, 1995.

Chen, S., W. A. Tolbert, and D. D. Dlott. <u>Journal of Physical Chemistry,</u> vol. 98, no. 7759, 1994.

Dlott, D. D., and M. D. Fayer. <u>Journal of Chemical Physics,</u> vol. 92, no. 3798, 1990.

Elert, M. L., D. M. Deaven, D. W. Brenner, and C. T. White. <u>Physical Review,</u> vol. B39, no. 1453, 1989.

Erpenbeck, J. J. <u>Physical Review,</u> vol. A46, no. 6406, 1992.

Fickett, W. <u>Introduction to Detonation.</u> Berkley: University of California Press, 1985.

Fickett, W., and W. C. Davis. <u>Detonation.</u> Berkley: University of California Press, 1979.

Fried, L. E., and A. J. Ruggiero. <u>Journal of Physical Chemistry,</u> vol. 98, no. 9786, 1994.

Gupta, Y. M., G. I. Pangilinan, J. M. Winey, and C. P. Constantinou. <u>Physics Letters,</u> vol. 232, no. 341, 1995.

Holian, B. L., W. G. Hoover, B. Moran, and G. K. Straub. <u>Physical Review,</u> vol. A22, no. 2798, 1980.

Hong, X., S. Chen, and D. D. Dlott. <u>Journal of Physical Chemistry,</u> vol. 99, no. 9102, 1995.

Karo, A. M., J. R. Hardy, and F. E. Walker. <u>Acta Astronautica,</u> vol. 5, no. 1041, 1978.

Kawakatsu, T., and A. Ueda. <u>Journal of the Physical Society of Japan,</u> vol. 57, no. 2955, 1988.

Kawakatsu, T., and A. Ueda. <u>Journal of the Physical Society of Japan,</u> vol. 58, no. 831, 1989.

Kawakatsu, T., T. Matsuda, and A. Ueda. Journal of the Physical Society of Japan, vol. 57, no. 1191, 1988.

Mallard, E., and H. LeChatelier. C. R. Hebd. Sceances Acad. Sci., vol. 93, no. 145, 1881.

Miller, W. H. and T. F. George. Journal of Chemical Physics, vol. 56, no. 5668, 1972.

Powell, J. D., and J. H. Batteh. Physical Review, vol. B20, no. 1398, 1979.

Powell, J. D., and J. H. Batteh. Journal of Applied Physics, vol. 51, no. 2050, 1980.

Press, W. H., B. P. Flannery, S. A. Teukolsky, and W. T. Vetterling. Numerical Recipes. Cambridge: Cambridge University Press, 1986.

Raff, L. M., and D. L. Thompson. Theory of Chemical Reaction Dynamics. Boca Raton, FL: Chemical Rubber, M. Baer (ed.), vol. 4 and references therein, 1985.

Rice, B. M., W. Mattson, J. Grosh, and S. F. Trevino. Physical Review, vol. A, in press.

Robertson, D. H., D. W. Brenner, M. L. Elert, and C. T. White. Shock Compression of Condensed Matter, Elsevier Science Publishers B. V., p. 123, 1992.

Tokmakoff, A., M. D. Fayer, and D. D. Dlott. Journal of Physical Chemistry, vol. 97, no. 1901, 1993.

Tsai, D. H. Journal of Chemical Physics, vol. 70, no. 1375, 1979.

Tsai, D. H., and S. F. Trevino. Physical Review, vol. A24, no. 2743, 1981.

Tsai, D. H. Chemistry and Physics of Energetic Materials. Kluwer Academic Publishers, S. N. Bulusu (ed.), pp. 195–227, 1990.

Tsai, D. H., and S. F. Trevino. Journal of Chemical Physics, vol. 81, no. 5636, 1984.

White, C. T., D. H. Robertson, M. L. Elert, and D. W. Brenner. Microscopic Simulations of Complex Hydrodynamic Phenomena. New York: Plenum Press, M. Mareschal and B. L. Holian (eds.), p. 111, 1992.

White, C. T., S. B. Sinnott, J. W. Mintmire, D. W. Brenner, and D. H. Robertson. International Journal of Quantum Chemistry Symposium, vol. 28, no. 129, 1994.

NO. OF COPIES	ORGANIZATION
2	DEFENSE TECHNICAL INFO CTR ATTN DTIC DDA 8725 JOHN J KINGMAN RD STE 0944 FT BELVOIR VA 22060-6218
1	DIRECTOR US ARMY RESEARCH LAB ATTN AMSRL OP SD TA 2800 POWDER MILL RD ADELPHI MD 20783-1145
3	DIRECTOR US ARMY RESEARCH LAB ATTN AMSRL OP SD TL 2800 POWDER MILL RD ADELPHI MD 20783-1145
1	DIRECTOR US ARMY RESEARCH LAB ATTN AMSRL OP SD TP 2800 POWDER MILL RD ADELPHI MD 20783-1145

ABERDEEN PROVING GROUND

5	DIR USARL ATTN AMSRL OP AP L (305)

NO. OF COPIES	ORGANIZATION	NO. OF COPIES	ORGANIZATION
1	HQDA ATTN SARD TT DR F MILTON PENTAGON WASHINGTON DC 20310-0103	1	OFFICE OF NAVAL RESEARCH DEPARTMENT OF THE NAVY ATTN R S MILLER CODE 432 800 N QUINCY STREET ARLINGTON VA 22217
1	HQDA ATTN SARD TT MR J APPEL PENTAGON WASHINGTON DC 20310-0103	1	COMMANDER NAVAL AIR SYSTEMS COMMAND ATTN J RAMNARACE AIR 54111C WASHINGTON DC 20360
1	HQDA OASA RDA ATTN DR C H CHURCH PENTAGON ROOM 3E486 WASHINGTON DC 20310-0103	2	COMMANDER NAVAL SURFACE WARFARE CENTER ATTN R BERNECKER R 13 G B WILMOT R 16 SILVER SPRING MD 20903-5000
4	COMMANDER US ARMY RESEARCH OFFICE ATTN R GHIRARDELLI D MANN R SINGLETON R SHAW P O BOX 12211 RSCH TRNGLE PK NC 27709-2211	5	COMMANDER NAVAL RESEARCH LABORATORY ATTN M C LIN J MCDONALD E ORAN J SHNUR R J DOYLE CODE 6110 WASHINGTON DC 20375
1	DIRECTOR ARMY RESEARCH OFFICE ATTN AMXRO RT IP LIB SERVICES P O BOX 12211 RSCH TRNGLE PK NC 27709-2211	2	COMMANDER NAVAL WEAPONS CENTER ATTN T BOGGS CODE 388 T PARR CODE 3895 CHINA LAKE CA 93555-6001
2	COMMANDER US ARMY ARDEC ATTN SMCAR AEE B D S DOWNS PCTNY ARSNL NJ 07806-5000	1	SUPERINTENDENT NAVAL POSTGRADUATE SCHOOL DEPT OF AERONAUTICS ATTN D W NETZER MONTEREY CA 93940
2	COMMANDER US ARMY ARDEC ATTN SMCAR AEE J A LANNON PCTNY ARSNL NJ 07806-5000	3	AL LSCF ATTN R CORLEY R GEISLER J LEVINE EDWARDS AFB CA 93523-5000
1	COMMANDER US ARMY ARDEC ATTN SMCAR AEE BR L HARRIS PCTNY ARSNL NJ 07806-5000	1	AFOSR ATTN J M TISHKOFF BOLLING AIR FORCE BASE WASHINGTON DC 20332
2	COMMANDER US ARMY MISSILE COMMAND ATTN AMSMI RD PR E A R MAYKUT AMSMI RD PR P R BETTS REDSTONE ARSENAL AL 35809		

NO. OF COPIES	ORGANIZATION	NO. OF COPIES	ORGANIZATION
1	OSD SDIO IST ATTN L CAVENY PENTAGON WASHINGTON DC 20301-7100	3	DIRECTOR SANDIA NATIONAL LABORATORIES DIVISION 8354 ATTN S JOHNSTON P MATTERN D STEPHENSON LIVERMORE CA 94550
1	COMMANDANT USAFAS ATTN ATSF TSM CN FORT SILL OK 73503-5600	1	BRIGHAM YOUNG UNIVERSITY DEPT OF CHEMICAL ENGINEERING ATTN M W BECKSTEAD PROVO UT 84058
1	UNIV OF DAYTON RSCH INSTITUTE ATTN D CAMPBELL AL PAP EDWARDS AFB CA 93523	1	CALIFORNIA INSTITUTE OF TECH JET PROPULSION LABORATORY ATTN L STRAND MS 125 224 4800 OAK GROVE DRIVE PASADENA CA 91109
1	NASA LANGLEY RESEARCH CENTER ATTN G B NORTHAM MS 168 LANGLEY STATION HAMPTON VA 23365	1	CALIFORNIA INSTITUTE OF TECHNOLOGY ATTN F E C CULICK MC 301 46 204 KARMAN LAB PASADENA CA 91125
4	NATIONAL BUREAU OF STANDARDS US DEPARTMENT OF COMMERCE ATTN J HASTIE M JACOX T KASHIWAGI H SEMERJIAN WASHINGTON DC 20234	1	UNIVERSITY OF CALIFORNIA LOS ALAMOS SCIENTIFIC LAB P O BOX 1663 MAIL STOP B216 LOS ALAMOS NM 87545
2	DIRECTOR LAWRENCE LIVERMORE NATIONAL LAB ATTN C WESTBROOK W TAO MS L 282 P O BOX 808 LIVERMORE CA 94550	1	UNIVERSITY OF CALIFORNIA BERKELEY CHEMISTRY DEPARMENT ATTN C BRADLEY MOORE 211 LEWIS HALL BERKELEY CA 94720
1	DIRECTOR LOS ALAMOS NATIONAL LAB ATTN B NICHOLS T7 MS B284 P O BOX 1663 LOS ALAMOS NM 87545	1	UNIVERSITY OF CALIFORNIA SAN DIEGO ATTN F A WILLIAMS AMES B010 LA JOLLA CA 92093
2	PRINCETON COMBUSTION RESEARCH LABORATORIES INC ATTN N A MESSINA M SUMMERFIELD PRINCETON CORPORATE PLAZA BLDG IV SUITE 119 11 DEERPARK DRIVE MONMOUTH JUNCTION NJ 08852	2	UNIV OF CALIFORNIA SANTA BARBARA QUANTUM INSTITUTE ATTN K SCHOFIELD M STEINBERG SANTA BARBARA CA 93106
		1	UNIV OF COLORADO AT BOULDER ENGINEERING CENTER ATTN J DAILY CAMPUS BOX 427 BOULDER CO 80309-0427

NO. OF COPIES	ORGANIZATION	NO. OF COPIES	ORGANIZATION
3	UNIV OF SOUTHERN CALIFORNIA DEPT OF CHEMISTRY ATTN R BEAUDET S BENSON C WITTIG LOS ANGELES CA 90007	4	PENNSYLVANIA STATE UNIVERSITY DEPT OF MECHANICAL ENGINEERING ATTN K KUO M MICCI S THYNELL V YANG UNIVERSITY PARK PA 16802
1	CORNELL UNIVERSITY DEPARTMENT OF CHEMISTRY ATTN T A COOL BAKER LABORATORY ITHACA NY 14853	2	PRINCETON UNIVERSITY FORRESTAL CAMPUS LIBRARY ATTN K BREZINSKY I GLASSMAN P O BOX 710 PRINCETON NJ 08540
1	UNIVERSITY OF DELAWARE CHEMISTRY DEPARTMENT ATTN T BRILL NEWARK DE 19711	1	PURDUE UNIVERSITY SCHL OF AERONAUTICS & ASTRONAUTICS ATTN J R OSBORN GRISSOM HALL WEST LAFAYETTE IN 47906
1	UNIVERSITY OF FLORIDA DEPT OF CHEMISTRY ATTN J WINEFORDNER GAINESVILLE FL 32611	1	PURDUE UNIVERSITY DEPARTMENT OF CHEMISTRY ATTN E GRANT WEST LAFAYETTE IN 47906
3	GEORGIA INSTITUTE OF TECHNOLOGY SCHOOL OF AEROSPACE ENGINEERING ATTN E PRICE W C STRAHLE B T ZINN ATLANTA GA 30332	2	PURDUE UNIVERSITY SCHL OF MECHANICAL ENGNRNG ATTN N M LAURENDEAU S N B MURTHY TSPC CHAFFEE HALL WEST LAFAYETTE IN 47906
1	UNIVERSITY OF ILLINOIS DEPT OF MECH ENG ATTN H KRIER 144MEB 1206 W GREEN ST URBANA IL 61801	1	RENSSELAER POLYTECHNIC INST DEPT OF CHEMICAL ENGINEERING ATTN A FONTIJN TROY NY 12181
1	THE JOHNS HOPKINS UNIV CPIA ATTN T W CHRISTIAN 10630 LITTLE PATUXENT PKWY SUITE 202 COLUMBIA MD 21044-3200	1	STANFORD UNIVERSITY DEPT OF MECHANICAL ENGINEERING ATTN R HANSON STANFORD CA 94305
1	UNIVERSITY OF MICHIGAN GAS DYNAMICS LAB ATTN G M FAETH AEROSPACE ENGINEERING BLDG ANN ARBOR MI 48109-2140	1	UNIVERSITY OF TEXAS DEPT OF CHEMISTRY ATTN W GARDINER AUSTIN TX 78712
1	UNIVERSITY OF MINNESOTA DEPT OF MECHANICAL ENGINEERING ATTN E FLETCHER MINNEAPOLIS MN 55455	1	VA POLYTECH INST AND STATE UNIV ATTN J A SCHETZ BLACKSBURG VA 24061

NO. OF COPIES	ORGANIZATION	NO. OF COPIES	ORGANIZATION
1	SCIENCE APPLICATIONS INC ATTN R B EDELMAN 23146 CUMORAH CREST WOODLAND HILLS CA 91364	1	UNIVERSAL PROPULSION COMPANY ATTN H J MCSPADDEN 25401 NORTH CENTRAL AVENUE PHOENIX AZ 85027-7837
3	SRI INTERNATIONAL ATTN G SMITH D CROSLEY D GOLDEN 333 RAVENSWOOD AVENUE MENLO PARK CA 94025	1	VERITAY TECHNOLOGY INC ATTN E B FISHER 4845 MILLERSPORT HIGHWAY EAST AMHERST NY 14051-0305
1	STEVENS INSTITUTE OF TECH DAVIDSON LABORATORY ATTN R MCALEVY III HOBOKEN NJ 07030	1	FREEDMAN ASSOCIATES ATTN E FREEDMAN 2411 DIANA ROAD BALTIMORE MD 21209-1525
1	SVERDRUP TECHNOLOGY INC LERC GROUP ATTN R J LOCKE MS SVR 2 2001 AEROSPACE PARKWAY BROOK PARK OH 44142	3	ALLIANT TECHSYSTEMS ATTN C CANDLAND L OSGOOD R BECKER 600 SECOND ST NE HOPKINS MN 55343
1	SVERDRUP TECHNOLOGY INC ATTN J DEUR 2001 AEROSPACE PARKWAY BROOK PARK OH 44142	1	DIRECTOR US ARMY BENET LABS ATTN SAM SOPOK AMSTRA AR CCB T WATERVLIET NY 12189
3	THIOKOL CORPORATION ELKTON DIVISION ATTN R BIDDLE R WILLER TECH LIB P O BOX 241 ELKTON MD 21921		
3	THIOKOL CORPORATION WASATCH DIVISION ATTN S J BENNETT P O BOX 524 BRIGHAM CITY UT 84302		
1	UNITED TECHNOLOGIES RSCH CENTER ATTN A C ECKBRETH EAST HARTFORD CT 06108		
1	UNITED TECHNOLOGIES CORP CHEMICAL SYSTEMS DIVISION ATTN R R MILLER P O BOX 49028 SAN JOSE CA 95161-9028		

NO. OF
COPIES ORGANIZATION

ABERDEEN PROVING GROUND

36   DIR USARL
        ATTN: AMSRL-WT-P, A HORST
                AMSRL-WT-PC,
                  R A FIFER
                  G F ADAMS
                  W R ANDERSON
                  R A BEYER
                  S W BUNTE
                  C F CHABALOWSKI
                  K P MCNEILL-BOONSTOPPEL
                  A COHEN
                  R CUMPTON
                  R DANIEL
                  D DEVYNCK
                  N F FELL
                  B E FORCH
                  J M HEIMERL
                  A J KOTLAR
                  M R MANAA
                  W F MCBRATNEY
                  K L MCNESBY
                  S V MEDLIN
                  M S MILLER
                  A W MIZIOLEK
                  S H MODIANO
                  J B MORRIS
                  J E NEWBERRY
                  S A NEWTON
                  R A PESCE-RODRIGUEZ
                  B M RICE
                  R C SAUSA
                  M A SCHROEDER
                  J A VANDERHOFF
                  M WENSING
                  A WHREN
                  J M WIDDER
                  C WILLIAMSON
                AMSRL-CI-CA, R PATEL

INTENTIONALLY LEFT BLANK.

USER EVALUATION SHEET/CHANGE OF ADDRESS

This Laboratory undertakes a continuing effort to improve the quality of the reports it publishes. Your comments/answers to the items/questions below will aid us in our efforts.

1. ARL Report Number __ARL-TR-981_____ Date of Report __March 1996_____

2. Date Report Received _____

3. Does this report satisfy a need? (Comment on purpose, related project, or other area of interest for which the report will be used.) _____

_____

_____

4. Specifically, how is the report being used? (Information source, design data, procedure, source of ideas, etc.) _____

_____

_____

5. Has the information in this report led to any quantitative savings as far as man-hours or dollars saved, operating costs avoided, or efficiencies achieved, etc? If so, please elaborate. _____

_____

_____

6. General Comments. What do you think should be changed to improve future reports? (Indicate changes to organization, technical content, format, etc.) _____

_____

_____

_____

Organization

CURRENT
ADDRESS   Name

                 Street or P.O. Box No.

                 City, State, Zip Code

7. If indicating a Change of Address or Address Correction, please provide the Current or Correct address above and the Old or Incorrect address below.

Organization

OLD   Name
ADDRESS
                 Street or P.O. Box No.

                 City, State, Zip Code

(Remove this sheet, fold as indicated, tape closed, and mail.)
(DO NOT STAPLE)
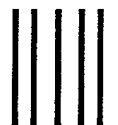
DEPARTMENT OF THE ARMY

OFFICIAL BUSINESS

BUSINESS REPLY MAIL
FIRST CLASS PERMIT NO 0001,APG,MD

POSTAGE WILL BE PAID BY ADDRESSEE

DIRECTOR
U.S. ARMY RESEARCH LABORATORY
ATTN: AMSRL-WT-PC
ABERDEEN PROVING GROUND, MD 21005-5066